SSIM 2025 - JJ Potter & J Wesseloo (eds)

doi:10.36487/ACG_repo/2535_36

A kinematic-based method to quickly inform operational decisions in response to slope deformation

Bijan Peik [a,*], **Kevin Azocar** [a], **Karl Lawrence** [a], **Serdar Ergun** [b]

[a] *Equilibrium Mining, USA*

[b] *Rio Tinto, USA*

Abstract

Open pit mining operations commonly use slope monitoring systems to detect and respond to unforeseen slope movement events. Following such events, detailed supporting investigations are initiated to assess the most likely cause(s) of the movement. Studies may include empirical, kinematic and/or numerical analyses, depending on the complexity of the mechanism and timeline for implementing any required engineering controls. In many cases this can be a time-consuming process; mine personnel would greatly benefit from having more immediate information to support operational and planning decisions while more detailed analyses are being conducted. This paper outlines an alternative kinematic-based method that can be used as an efficient initial assessment of the primary controls associated with an interpreted or conceptual failure surface. In this approach, reasonable or extreme percentile ranges of select inputs such as material strength, pore pressure and structural orientation are first defined. The Factor of Safety (FOS) is then evaluated along the defined slip surface by sampling within the bounds of the data. By evaluating the parameter sensitivity of the FOS, the most probable critical controls can be identified given local conditions, and mitigation options can be quickly evaluated. Conceptual examples along with a large-scale case study using the Leo failure at Rio Tinto's Bingham Canyon Mine are presented to demonstrate the details and advantages of the approach.

Keywords: *3D kinematics, slope optimisation, failure mechanism*

1 Introduction

Open pit mines globally utilise slope monitoring systems to support operational decisions, evaluate engineering designs against performance and maintain safe working conditions for mining personnel. When slope movements occur, real-time performance metrics with sub-millimetre-scale accuracy are available to operations for making informed decisions and implementing thorough trigger action response plans reflective of the level of risk (e.g. Bakken et al. 2020). The short-term response plan is often followed by more detailed supporting investigations to evaluate the most likely cause of the movement event.

The amount and availability of site-based data at many operating mines support in-depth investigations of deforming areas of the slope, so the underlying critical controls and the potential project risks (safety, operational and financial) can be identified. A collection of geotechnical analysis options, including empirical, kinematic and numerical methods, are commonly used to assist in this interpretation through back-analysis and predictive simulation to inform risk. The selected method depends on the type and complexity of the potential failure mechanism. For example, for structurally controlled bench-scale mechanisms, kinematic analyses using commercially available tools such as SWedge (RocScience 2023a) or RocPlane (RocScience 2023b) are commonly used. For larger-scale mechanisms, 2D and 3D limit equilibrium tools may be selected for initial analyses, given their relative ease of use. As the complexity increases, 2D and 3D numerical stress modelling may be warranted using continuum, discontinuum or hybrid methods – each with specific

[*] Corresponding author. Email address: bpeik@equilibriummining.com

capabilities, such as advanced constitutive models incorporating discrete fracture networks, coupling options, etc. (e.g. Ergun et al. 2023).

For simple mechanisms, analyses can be conducted relatively quickly using one of the above methods. However, as the mechanism becomes larger and more complex, the analyses become more time-consuming and require a higher level of experience to interrogate results. A wider comprehensive understanding of the failure mechanism is often gained later in more detailed design studies, but this does not provide insight into critical controls (and the impact of mitigation alternatives) on a shorter timeframe when mine personnel need to make operational decisions.

This paper outlines an alternative kinematic-based approach that can be used to efficiently assess the primary controls associated with a failure surface for a slope movement event. It requires an interpreted or conceptual 3D slip surface, but multiple surfaces can be used in the early stages of the investigation where significant uncertainty remains. The shape can be a simple rock block or series of blocks, a step-path mechanism with undulating surfaces, a non-daylighting wedge or any other geometry that is supported by field observations. This approach can be used to support critical project decisions as part of a failure investigation, or to evaluate potential mitigation options (buttressing, redesign/step-out, depressurisation, etc.). It can also be used to identify critical components of complex mechanisms prior to detailed stress modelling studies, helping to inform key variables and drivers of the failure (i.e. weak rock mass or faults, pore pressure or anisotropy).

One of the primary advantages of this method is the speed at which the analysis can be completed – the computation time generally ranges from milliseconds for simple input data to minutes for more complex scenarios. Furthermore, 3D input data (if available) is fully supported, inclusive of static or transient pore pressure grids, stress distributions from existing numerical models, geotechnical block models (rock mass rating, geological strength index (GSI), uniaxial compressive strength (UCS), etc.), or geology wireframes. The subsequent sections will provide details on the methodology and illustrate the approach using conceptual examples and a case study at the Bingham Canyon Mine in Utah, USA.

2 Methodology

For ease of reference, the approach is referred to as the critical component analysis (CCA) throughout the remainder of this paper. The objective of the CCA framework is to provide a high-level overall assessment of potential failure mechanisms, including the relative impact and (quantifiable) contribution of each component. This can also provide insight into whether the conceptual understanding is flawed in any way or requires further development. In general, the CCA aims to provide answers to the following questions:

- Given the understanding of the conceptual mechanism, what is the range of parameters (strength, pore pressure, etc.) that permit the mechanism to fail? Does that range of parameters fall within reasonable bounds based upon the current geotechnical understanding?
- For mechanisms with multiple controls (rock mass, discontinuity strength, pore pressure, etc.), what is the relative impact of each on the computed Factor of Safety (FOS) and interpreted failure mechanism?
- What is the likelihood of failure given the conceptual understanding, key variables and assumed uncertainty? How does that change based upon input assumptions?

Figure 1 displays a general operational support workflow incorporating the CCA as a valuable link between the ongoing geotechnical activities (such as characterisation and monitoring) and operational decisions following a movement event.

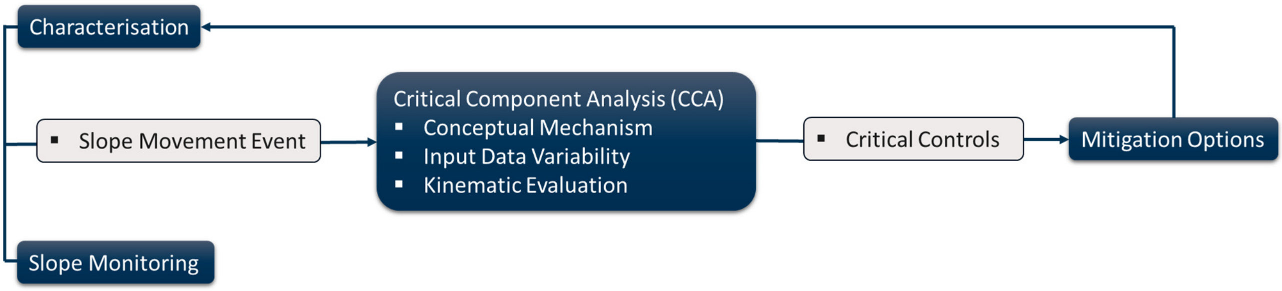

Figure 1 Critical component analysis workflow in operational support

The key input and process assumptions for the CCA evaluation displayed in Figure 1are described as follows:

- Conceptual mechanism: assumptions from a conceptual understanding of the mechanism, informed by available site data and monitoring, should be used to create an interpreted 3D failure mechanism/slip surface. If warranted, several failure surfaces can be provided to assess the uncertainty in extent, depth and overall size
- Input data variability: given the potential controls on the mechanism (i.e. rock mass strength, fault strength, discontinuity orientation/strength, pore pressure), deterministic values and the uncertainty of each parameter should be defined. This can be a rough estimate or more detailed, depending on the site knowledge and available supporting data. The range of variability can also be referred to as the parameter space of the potential failure mechanism
- Kinematic evaluation: the method for estimating the stability margin (or FOS) in the CCA is based on a kinematic evaluation of composite failure mechanisms (i.e. those shearing through a combination of rock mass and/or discontinuities), first introduced by Lawrence et al. (2020) and applied in subsequent publications (e.g. Valerio et al. 2020 and Veltin et al. 2023). The accuracy and computational efficiency of this method is comparable to other commonly used kinematic tools, but without the limitation that blocks or mechanisms must be kinematically admissible or removable. This allows for complex failure mechanisms to be evaluated quickly to gain operational insight prior to moving to more robust stress modelling options.

The CCA framework combines a conceptual understanding of the mechanism, options for potential failure surfaces, the defined input data variability and the kinematic-based FOS evaluation to provide insight into the critical controls. The process of evaluation is comparable to other sensitivity-type analyses, where the extent of the parameter space is evaluated to assess the impact of each variable on the results. In fact, the assumptions and processes from response surface methods (Myers et al. 2016), commonly applied to assess the probability of failure in 3D stress modelling (e.g. Ortiz et al. 2015), are used as the starting point for the analysis.

The authors highlight that a key assumption in applying this methodology is that the failure mechanism is reasonably well understood and the failure surface can be defined or interpreted. When uncertainty is high, the applicability of this approach, as with any approach in fact, should be assessed to understand the limitations.

3 Demonstration of approach

To illustrate the CCA framework, two conceptual examples with known controls are presented, each with an increasing level of complexity. The examples presented are manufactured to demonstrate the approach and are not meant to infer that these mechanisms could not be evaluated with other tools or approaches. Several ways of looking at the results will be presented, each providing a slightly different perspective into the critical controls.

3.1 Daylighting wedge

A inter-ramp scale daylighting wedge is considered, displayed in Figure 2. Both the left and right releases are assumed to be variable faults characterised by Hoek–Brown parameters – meant to represent average or typical values for the rock mass being analysed. Note that this is unlikely for a mechanism of this scale but helpful for illustration purposes.

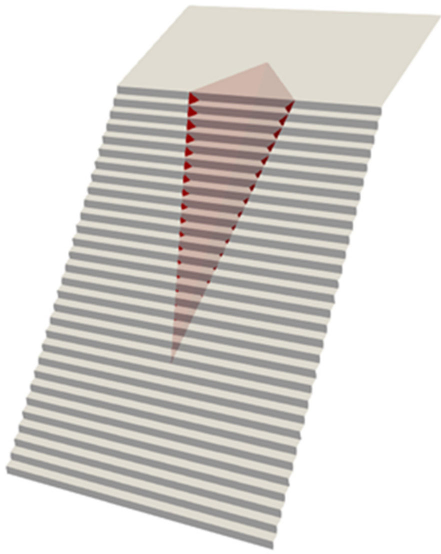

Figure 2 Daylighting wedge on an inter-ramp slope

The Hoek–Brown parameters and slope dimensions used for this case are provided in Table 1. The failure surface (two faces forming the slip planes of the wedge) is provided as the interpreted mechanism, with the conceptual understanding that the Hoek–Brown rock mass strength and pore pressure are likely contributing factors. It is assumed that the shape, size, and conceptual failure mechanism have been informed by site knowledge or a combination of knowledge and monitoring data (i.e. radar deformation limits, prisms, etc.).

Table 1 Slope dimensions and Hoek–Brown rock mass parameters

Slope dimensions		Rock mass properties	
Slope height (m)	460	Density (kg/m^3)	2,450
Slope angle (°)	37	Geological strength index	40
Bench width (m)	15	m_i	11
Bench face angle (°)	68	Uniaxial compressive strength (MPa)	14
Bench height (m)	50	Disturbance factor (D)	1

Estimated ranges for the input data variability are provided in Table 2 with the m_i and disturbance factor not varied in this example. These do not need to be precise, and it is recommended that the engineer purposely choose extreme limits. By taking this approach, the impact of each variable can be evaluated and potentially eliminated if results are outside a reasonable range, as informed by engineering judgement and local site knowledge.

Table 2 Deterministic values and parameter space assumptions for a simple daylighting wedge

Input parameters	Representative value (average or typical)	Relative variability range
Uniaxial compressive strength	14	50–100 (%)
Geological strength index	40	50–100 (%)
m_i	11	50–100 (%)
Pore pressure (Ru*)	0	0–0.4

* Pore pressure as a function of overburden, 0.4 ~ hydrostatic

For the daylighting wedge, the CCA framework computes the impact of each variable independently by evaluating the FOS for the mechanism at equally spaced (user defined, 10 intervals selected in this example) intervals within the parameter space of each variable, keeping all other parameters fixed at their deterministic values. This first process defines the "response" (as defined in response surface methods) of the mechanism to each variable change. This permits calculation of the probability of failure (for a specific failure mechanism) by sampling from the known distribution of input variables and computing the FOS for each sample by scaling each parameter relative to its mean response using a response function (F), i.e Equation 1:

$$FOS_{Sam} = FOS_{Det} \times F1_{UCS} \times F2_{GSI} \times F3_{mi} \times F4_{Ru} \quad (1)$$

Where F1 through F4 are the response functions of each variable, and the subscripts *Det* and *Sam* refer to the deterministic and sample FOS values, respectively.

The individual response of the different parameters is readily observable in Figure 3a. For example, the reduction in GSI and UCS to 50% of their deterministic values reduces the FOS to approximately 1.25 and 0.75, respectively, when varied independently. The relative impact of each variable on the computed FOS when independently varied to the limit of the parameter space is illustrated in Figure 3b. This graph highlights the relative magnitude of the impact of each variable in comparison to initial properties, without considering failure (i.e. the impact presented on the X-axis of Figure 3b could indicate that the FOS decreases 50% relative to an FOS = 2.5). Figure 3b highlights that, independently, GSI has the largest impact on the computed FOS for the given parameter space.

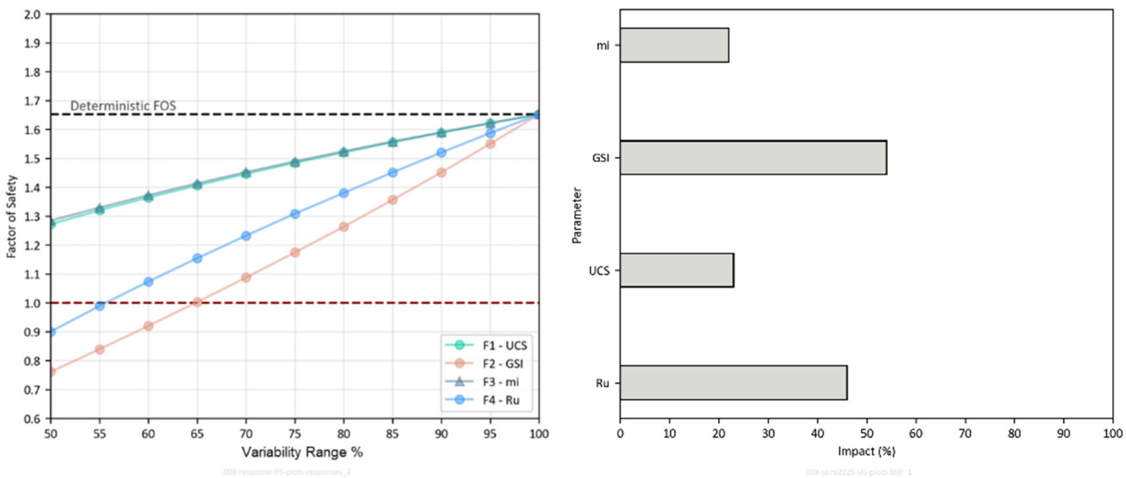

(a) (b)

Figure 3 (a) Individual response functions of each variable; (b) Relative impact of each variable on the computed Factor of Safety for the daylighting wedge example

To further understand the dependency of the failure mechanism on key variables, the response is also evaluated by assessing pair-wise combinations of parameters. This is illustrated in Figures 4a to 4f using contour maps to show the change in FOS as the pair-wise combinations of parameters are varied within their parameter spaces (with all other parameters fixed).

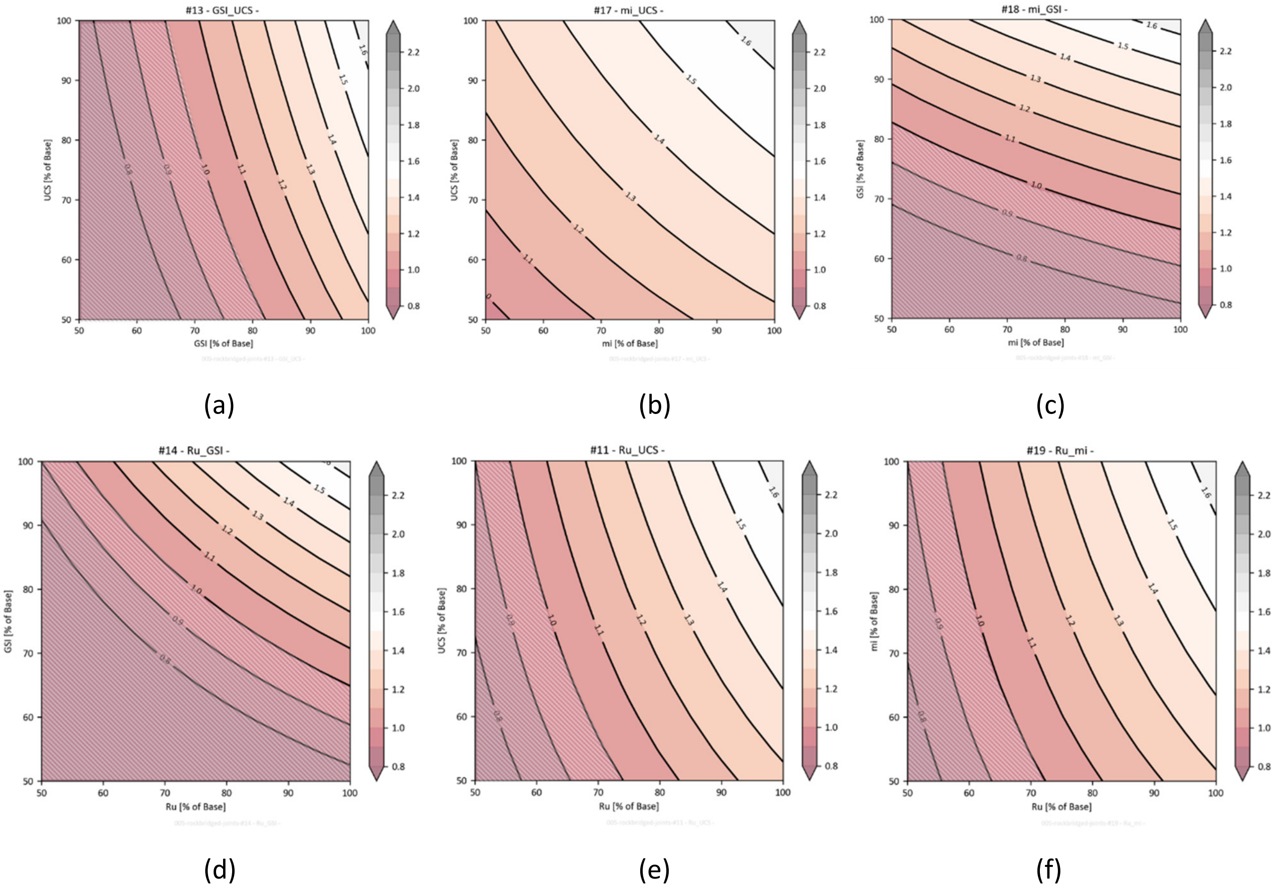

Figure 4 Factor of Safety (FOS) contour map showing the impact of: (a) Geological strength index (GSI) and uniaxial compressive strength (UCS); (b) m_i and UCS; (c) m_i and GSI; (d) Pore pressure (Ru) and GSI; (e) Ru and UCS; (f) Ru and m_i when considered concurrently in the daylighting wedge case – the area below FOS = 1.0 is highlighted

The upper right corner of the plot represents the FOS where the two assessed parameters are fixed at their deterministic values. The area below FOS = 1.0 is highlighted with transparent hatching in Figure 4 to illustrate the proportion of the parameter space which results in failure (FOS < 1.0) – the larger the area, the more critical the combined parameters are to the response. For example, with a 50% reduction in UCS or m_i individually (Figure 4b), the FOS does not fall below 1.0 but, at their combined lower bound, the FOS is below 1.0. Figure 4d highlights that the FOS is very sensitive to a combination of GSI and Ru – approximately 63% of the area (parameter space) is below the FOS = 1.0 contour – and the more closely spaced contour lines indicate a higher FOS gradient as each parameter is reduced. Other observations that can be made from these plots include:

- A GSI reduction to ~70–80% of its deterministic value yields an FOS near 1.0 (for any value of UCS in the parameter space) per Figure 5a.
- m_i has less of an impact on FOS when varied in combination with UCS.
- Pore pressure also has a significant impact on FOS – though the computed FOS is less sensitive to pore pressure in comparison to GSI.

- The displayed plots show non-linear contours which is reasonable, particularly when complex failure mechanisms develop through multiple rock mass units characterised by non-linear failure envelopes. When the plots show linear contours, the single variable response function is considered a reasonable response estimate.

Table 3 shows the relative impact of each variable independently, and in combination with other variables, by computing the percentage of the parameter space with an FOS < 1.0. The table is colour-coded based upon the relative change in FOS when varying the parameters, with a scale of low (0 to 5%), moderate (5 to 25%) and high (greater than 25%). These ranges can be revised as necessary. The diagonals of the table represent the impact of the variables independently, which for single response variables (as provided in Figure 3) is computed as the portion of the FOS line below 1.0.

It is evident from Figure 5 that GSI and Ru have the largest impact on results, with other variables (UCS, m_i) having comparatively less impact (unless combined with GSI and/or Ru). This should not be interpreted to infer decisively that the failure mechanism could not be formed with one of these less likely parameters (as it will depend on local mine site conditions and spatial variation). This process is meant to identify the potential components of the failure mechanism, given the uncertainty ranges provided by the engineer. The objective is to provide insight quickly and efficiently to support operational decisions or to reduce sensitivities being evaluated in other tools to those most likely to replicate the slope performance.

Table 3 Maximum impact of each variable (or pair of variables) as a per cent of the parameter space which permits failure (Factory of Safety < 1) for the daylighting wedge case

Sensitivity	UCS	GSI	m_i	Ru
Uniaxial compressive strength (UCS)	0	45	1	27
Geological strength index (GSI)	–	30	46	63
m_i	–	–	0	25
Pore pressure (Ru)	–	–	–	12

Low	Moderate	High
0 – 5%	5 – 25%	25% +

3.2 Non-daylighting wedge with major fault and joint control

The second example extends the previous simple wedge case to a more realistic scenario, where the left and right release are controlled by discontinuities (i.e. joint set, fault or bedding), and the conceptual sliding planes are steepened so that the wedge no longer daylights the slope. In this case, the mechanism is required to break through rock mass at the toe as shown in Figure 6. It is assumed that the left release of the wedge is controlled by less persistent discontinuities such as a joint set (with rock bridge), and the right release is controlled by a major fault with higher persistence (no rock bridge).

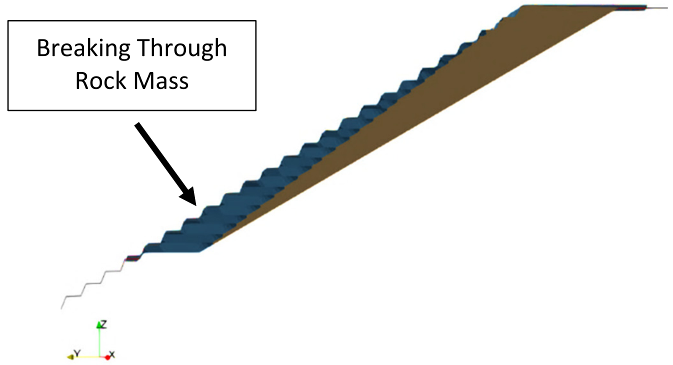

Figure 6 Side view of the non-daylighting wedge along with the rock mass component shown in blue

The deterministic input values and ranges for this case are summarised in Table 4, now including Mohr–Coulomb discontinuity strength properties and rock bridge assumptions.

Table 4 Deterministic values and parameter space assumptions for a non-daylighting wedge, with sliding along a joint set on the right release and sliding along a fault on the right release

Input parameters	Representative value (average)	Variability range (%)
Uniaxial compressive strength	30 MPa	50–100
Geological strength index	40	5–100
m_i	11	Not varied
Disturbance factor (D)	1.0	Not varied
Pore pressure (Ru)	0	0–0.4
Fault strength (cohesion/ friction)	700 kPa/20°	50–100
Fault orientation (dip/dip direction)	40°/025°	Not varied
Joint set strength (cohesion/ friction)	500 kPa/27°	50–100
Joint set rock bridge	5%	Not varied
Joint set orientation (dip/dip direction)	40°/295°	Not varied

The rock bridging in this example is fixed at 5% for the joint set. The fault is assumed to be a major, persistent inter-ramp scale structure, so no rock bridging is applied. The joint orientation is fixed as both the left and right releases are assumed to exploit these orientations from the conceptual failure surface. In more complex scenarios where failure mechanisms are composed of multiple structural domains and/or geological units, this can be extended to use multiple joint sets and orientation ranges, providing additional insight into mechanism controls.

Figures 7a and b present the individual response functions of each variable along with relative impact of each variable, respectively, on the FOS over the extents of the parameter space. Figure 7c presents the impact of each variable, and pairs of variables, on the potential for failure (FOS < 1) for the non-daylighting wedge case. The following observations are noted:

- The impact of pore pressure is significant, illustrating that the impact on FOS is approximately three times higher than the joint and fault strengths over the assumed parameter ranges. It also amplifies the impact of other parameters, as shown in Figure 7.
- Compared to the daylighting wedge case, the impact of rock mass strength has decreased, primarily due to the change in the conceptual interpretation of the mechanism (i.e. addition of structural releases), but GSI still has a small impact on the FOS through the rock-bridged joint strength assumptions and the requirement that the non-daylighting wedge breaks through the rock mass at the toe.
- Joint strength assumptions have a slightly larger impact in comparison to the fault strength assumptions.

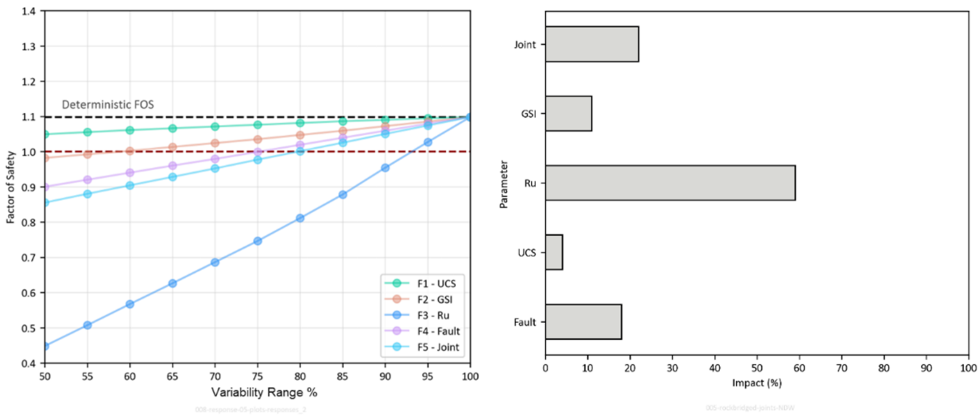

(a) (b)

Sensitivity	UCS	GSI	Ru	Joint	Fault
UCS	0	31	89	62	69
GSI	–	18	94	80	84
Ru	–	–	86	96	97
Joint	–	–	–	50	90
Fault	–	–	–	–	59

Low	0 – 5%
Moderate	5 – 25%
High	25% +

(c)

Figure 7 (a) Individual response functions of each variable; (b) Relative impact of each variable on the computed Factor of Safety (FOS); (c) Maximum impact of each variable (or pair of variables) as a per cent of the parameter space which permits failure (FOS < 1) for the non-daylighting wedge case

Knowledge of the possible critical controls provides quick, valuable information to operations to make an informed evaluation of potential failure mitigation options. For this case, given the significant impact of water on the FOS, depressurisation measures in the movement area would be a reasonable mitigation option to consider. Deterministically, the movement area is assumed to be dry, but the analyses indicate that increases in water, for example during snow melt or rainfall events, could trigger a significant response.

The joint and fault releases were also identified as having a significant impact on FOS. Independently, their impact is less significant compared to water, as shown in Figure 7a, while in combination with water, the impact is amplified. To reduce the impact of these releases on the movement mechanism, another reasonable mitigation option would be to install a buttress or step-out at the toe of the moving block. The objective here is to provide additional resistance against sliding and increase the amount of rock at the toe that the non-daylighting wedge must break through.

4 Case study

The conceptual examples in the previous sections describe how the CCA framework can rapidly identify key controls in slope failure mechanisms of varying complexity. While these simplified scenarios serve to demonstrate the methodology and outputs of the approach, the real strength of CCA lies in its ability to assess more complex, large-scale slope instabilities with geologically realistic and heterogeneous input conditions. To illustrate this, the CCA framework was applied to the Leo failure – a well-documented and complex inter-ramp scale instability that occurred along the south wall of the at the Bingham Canyon Mine that was previously analysed in detail by Ergun et al. (2023). The failure mechanism involved a combination of structurally controlled releases through fault and anisotropy, breaking through weak rock mass in the toe. Figure 8a displays a view of the Bingham Canyon Mine south wall (post Leo failure), with Figure 8b highlighting the interpreted Leo failure scarp and pre-failure topography.

(a) (b)

Figure 8 (a) Bingham Canyon Mine south wall on 31 May 2021, prior to the Leo failure; (b) Post failure (Ergun et al. 2023)

The complete geology with defined geotechnical units (GTUs) at Bingham Canyon Mine, together with detailed rock mass and fault strengths, were used in this case study. Multiple anisotropy types (bedding, joint, fault) and orientation/strength were permitted within each GTU. 3D pore pressure grids from calibrated models were used to inform groundwater conditions, with transient conditions evaluated using an applied Ru approach. To facilitate application of the CCA framework, all input parameters were exported into a block model format (comma-separated value file). Figure 9 displays the Leo conceptual failure surface coloured by geology, the GSI block model and faults.

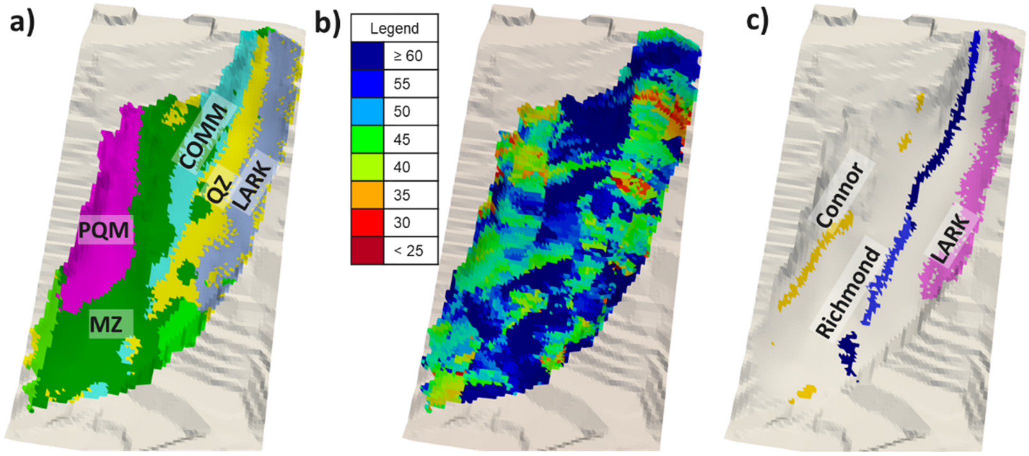

Figure 9 The Leo failure surface used in the critical component analysis tool, coloured by (a) geology, (b) geological strength index, and (c) faults

Rock mass, fault and anisotropy strengths were permitted to vary by up to ± 50%. The anisotropy orientation was permitted to vary by up to 15° in dip and 50° in dip direction. As multiple anisotropies/sets are observed within each rock mass, the orientation of the conceptual failure surface (which discretised into many triangles) is used to select the critical set (and associated strengths) in the analysis. The Ru assumptions varied between 0.0 to 0.4 to evaluate the impact of the extreme pore pressure assumptions.

Figure 10 displays the relative impact of each variable on the FOS over the extents of the parameter space, along with the impact of each variable and pairs of variables.

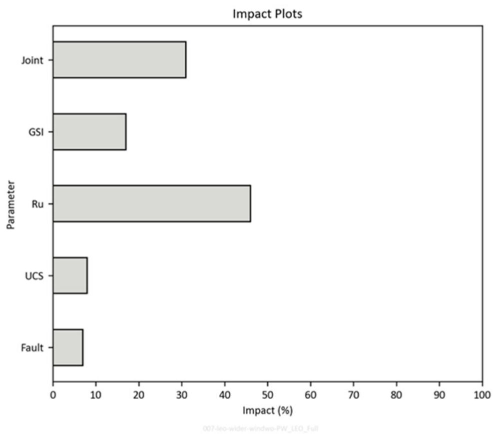

Sensitivity	UCS	GSI	Ru	Fault	Joint
UCS	0	45	77	1	67
GSI	–	33	91	57	87
Ru	–	–	69	75	92
Fault	–	–	–	0	65
Joint	–	–	–	–	54

Ru varied between 0.0 to 0.40

Low	Moderate	High
0 – 5%	5 – 25%	25% +

(a) (b)

Figure 10 (a) Individual response functions of each variable; (b) Maximum impact of each variable (or pair of variables) as a per cent of the parameter space which permits failure (Factory of Safety < 1) for the Leo mechanism

Multiple components display significant impact on the mechanism: (i) Ru assumptions provide the highest impact and amplify the impact of other parameters, and (ii) joint strength assumptions display a significantly larger impact in comparison to the fault and rock mass strength assumptions. To better isolate the critical controls of the mechanism, the pore pressure assumptions were limited to a reasonable range (Ru = 0–0.05) based on field observations that ,at the time of failure, the slope was relatively dry and without any major precipitation. Figure 11 displays the CCA results for the case with the Ru limited to more reasonable ranges.

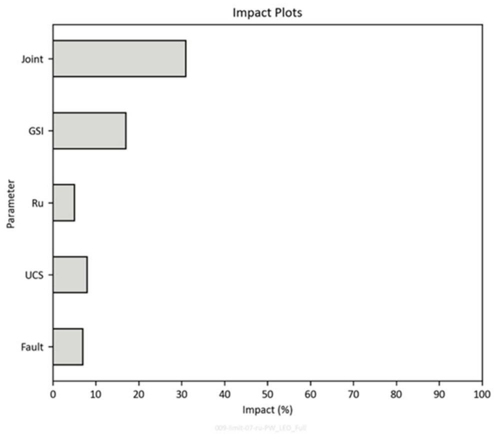

(a)

Sensitivity	UCS	GSI	Ru	Fault	Joint
UCS	0	45	0	1	67
GSI	–	33	50	57	87
Ru	–	–	0	0	61
Fault	–	–	–	0	65
Joint	–	–	–	–	54

Ru varied between 0.0 to 0.05

Low	Moderate	High
0 – 5%	5 – 25%	25% +

(b)

Figure 11 (a) Individual response functions of each variable; (b) Maximum impact of each variable (or pair of variables) as a per cent of the parameter space which permits failure (Factor of Safety < 1) for the Leo mechanism with limited Ru variation

With restricted Ru ranges, the impact of UCS and fault strength is low when considered independently, with GSI and joint strength having a larger impact on FOS. The joint strength independently has the largest impact (Figure 11a), and this impact is amplified when combined with any other parameter (UCS, GSI, Ru or fault strength all having greater than 54% of results with FOS < 1.0).

To isolate the impact of GSI and illustrate how the approach can be used to investigate perturbations of the conceptual failure mechanism, anisotropy was completely removed from the CCA (no failure through anisotropy is permitted). Figure 12 displays the results for this scenario – GSI still has the largest impact on FOS (Figure 12a) but within the defined (extreme) parameter space of GSI, failure is not possible (i.e. FOS > 1.0 for all pair-wise combinations).

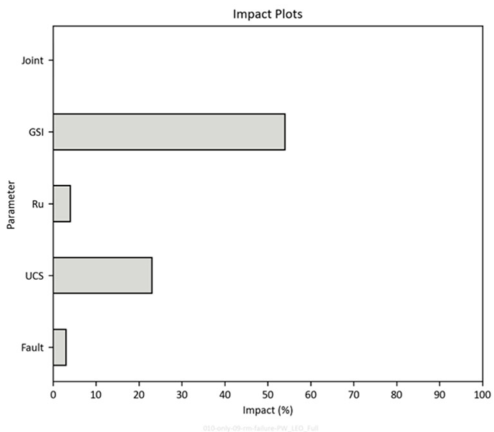

(a)

Sensitivity	UCS	GSI	Ru	Fault	Joint
UCS	0	0	0	0	No Anisotropy Considered
GSI	–	0	0	0	
Ru	–	–	0	0	
Fault	–	–	–	0	
Joint	–	–	–	–	

Ru varied between 0.0 to 0.05

Low	Moderate	High
0 – 5%	5 – 25%	25% +

(b)

Figure 12 (a) Individual response functions of each variable; (b) Maximum impact of each variable (or pair of variables) as a per cent of the parameter space which permits failure (Factor of Safety < 1) for the Leo mechanism with anisotropy disabled

The lowest FOS computed (FOS = 1.075) was achieved when both GSI and UCS were reduced by 50%, indicating that rock mass alone is unlikely to be the critical component of the observed Leo failure. Figure 13 displays the results for this same case, but when Ru was permitted to vary of the full range (Ru = 0.0–0.4), even though it is not supported by field observations.

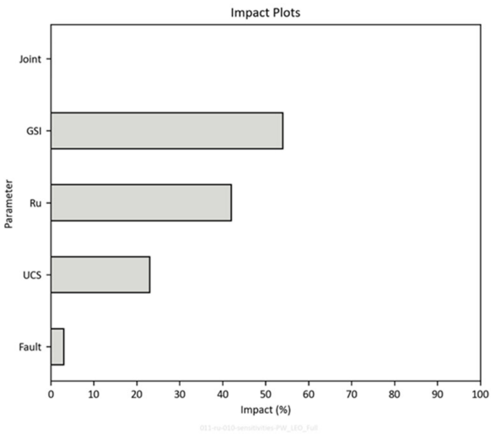

Sensitivity	UCS	GSI	Ru	Fault	Joint
UCS	0	0	0	0	No Anisotropy Considered
GSI	–	0	13	0	
Ru	–	–	0	0	
Fault	–	–	–	0	
Joint	–	–	–	–	

Ru varied between 0.0 to 0.40

Low	Moderate	High
0 – 5%	5 – 25%	25% +

(a) (b)

Figure 13 (a) Individual response functions of each variable; (b) Maximum impact of each variable (or pair of variables) as a per cent of the parameter space which permits failure (Factor of Safety < 1) for the Leo mechanism with anisotropy disabled with Ru range (Ru = 0.0 – 0.4)

With high Ru assumptions (Ru = 0.4) and a 50% reduction in GSI, only 13% of the trials resulted in FOS < 1.0. These two sensitivities (Figures 12 and 13) further support field observations that anisotropy is one of the critical components of the mechanism, and a mechanism exploiting ONLY weak rock mass and/or high pore pressure is unlikely to have led to the observed failure. This important learning can be used to guide the geotechnical investigations and forward work to consider a more detailed characterisation and mapping of the area.

This case study benefits from the detailed monitoring, field investigation and analyses conducted during and after the Leo failure (Ergun et al. 2022, 2023). The findings discussed above (anisotropy, faults and GSI as components of the Leo failure mechanism) are consistent with detailed, multi-year FLAC3D analyses completed by multiple consultants (Ergun et al. 2023). Findings from Ergun et al. (2023) indicated that the Leo failure was initiated by shearing along Lark Fault in the west and propagating through unfavourable anisotropy in the sediments and intrusive units in the east. GSI was incorporated through a detailed block model which reduced the uncertainty associated with this variable (as spatial variability is partially accounted for). Rock mass strength and pore pressure are considered to have played minor roles in the failure, though isolated damage zones around geological contacts exist – with the Leo mechanism dominated by the Lark Fault and shearing through anisotropy – that are consistent with learnings from the previous analyses.

5 Conclusion

The CCA framework provides a rapid and practical approach to evaluate the primary controls in small- to large-scale mechanisms using available geotechnical data and conceptual failure surfaces. The required inputs for this approach include a conceptual failure mechanism informed by the site monitoring data, and available characterisation. Different ranges of parameter variability can be assumed to evaluate the impact of each parameter individually or paired with other parameters. The current geotechnical understanding, along with the responses derived from CCA, allow engineers to identify the key controls, likelihood of conditions and the variables which have the highest impact on FOS.

Simple examples were provided to illustrate the required input and associated results. To illustrate the application in a mining environment, the CCA approach was applied to the Leo failure at Bingham Canyon Mine. The case study demonstrates that the CCA can effectively identify critical controls without detailed engineering analysis. The conclusions from the CCA are consistent with those identified through detailed numerical stress modelling and site observations but are available to inform decisions with 1–2 hours (as opposed to months). Key advantages of the CCA approach include its speed, flexibility in input complexity and intuitive visualisation of parameter sensitivity, enabling informed decision-making and targeted investigation. The ability to work directly with block model data and integrate 3D topography and mapping data further enhance its utility for operational teams. By providing timely insight into the most likely controls (and relative impact of mitigation measures), CCA supports more effective mitigation planning and prioritisation of geotechnical investigations. This framework is now being actively evaluated at additional sites to assess its broader application to other inter-ramp instabilities across varied geological and operational settings. Note that the CCA framework is another tool that can be used to efficiently interrogate and inform controls related to areas of increased deformation or instability in operating mines and is not considered a replacement for any of the other numerical, analytical, empirical or observational approaches already considered in the industry. It simply provides additional insight that can be used to inform operational risk during the early stages of a failure investigation while more detailed studies are being considered.

References

Bakken, KM, Chapin, GK & Abrahams, MG 2020, 'Trigger action response plan development and optimisation at the Bingham Canyon Mine', in PM Dight (ed.), *Slope Stability 2020: Proceedings of the 2020 International Symposium on Slope Stability in Open Pit Mining and Civil Engineering*, Australian Centre for Geomechanics, Perth, pp. 177–190, https://doi.org/10.36487/ACG_repo/2025_07

Ergun, S, Cambio, D, Williams, CP, Gaida, M, Lawrence, K, Katsaga, T, Lorig, L, Weigel, J, Gibbs, J, Chapin, G, Peik, B & Sankhaneel, S 2023, 'Back-analysis of the Bingham Canyon Mine southeast wall: a complex slope failure mechanism called Leo', in PM Dight (ed.), *SSIM 2023: Third International Slope Stability in Mining Conference*, Australian Centre for Geomechanics, Perth, pp. 559–576, https://doi.org/10.36487/ACG_repo/2335_37

Ergun, S, Emam, S, Rodriguez, P, Fahle, L, Schafer, K, Dedecker, F, ... Ross, B 2022, 'Particle flow code modelling of slope failure and runout at Bingham Canyon Mine', in I Barton & J Kemeny (eds), *Proceedings of the Slope Stability Symposium 2022*, Geotechnical Center of Excellence, The University of Arizona, Tucson.

Lawrence, KP, Nelson, MD, Yetisir, M & Matlashewski, P 2020, 'Kinematic assessment of composite failure mechanisms in pit slopes – a novel slip surface identification algorithm for DFN models', *Proceedings of the 54th US Rock Mechanics/Geomechanics Symposium,* American Rock Mechanics Association, Alexandria, pp. 559–576.

Myers, RH, Montgomery, DC & Anderson-Cook, CM 2016, *Response Surface Methodology: Process and Product Optimization using Designed Experiments*, 4th edn, John Wiley & Sons, Hoboken.

Ortiz, R, Silva, GR & Michalak, N 2015, 'Application of the response surface methodology to 3DEC analysis of open pit slopes', *Proceedings of the ISRM Regional Symposium – IX South American Congress on Rock Mechanics*, Sociedad Argentina de Mecánica de Rocas, Buenos Aires

Rocscience Inc 2023a, *SWedge: Surface Wedge Analysis for Slopes*, computer software, Rocscience Inc, Toronto, https://www.rocscience.com/software/swedge

Rocscience Inc 2023b, *RocPlane: Planar Wedge Analysis for Slopes*, computer software, Rocscience Inc, Toronto, https://www.rocscience.com/software/rocplane

Valerio, M, Rogers, S, Lawrence, KP, Moffitt, KM, Rysdahl, B & Gaida, M 2020, 'Discrete fracture network based approaches to assessing inter-ramp design', in PM Dight (ed.), *Slope Stability 2020: Proceedings of the 2020 International Symposium on Slope Stability in Open Pit Mining and Civil Engineering*, Australian Centre for Geomechanics, Perth, pp. 1017–1030, https://doi.org/10.36487/ACG_repo/2025_67

Veltin, KG, Peik, B & Lawrence, K 2023, 'A new approach to identify and analyse key blocks in pit slopes', in PM Dight (ed.), *SSIM 2023: Third International Slope Stability in Mining Conference*, Australian Centre for Geomechanics, Perth, pp. 939–950, https://doi.org/10.36487/ACG_repo/2335_64